Journal of Pharmaceutical Research International

33(18): 53-67, 2021; Article no.JPRI.66721
ISSN: 2456-9119
(Past name: British Journal of Pharmaceutical Research, Past ISSN: 2231-2919, NLM ID: 101631759)

Design of Guggul Lipid Loaded Chitosan Nanoparticles Using Box-Behnken Design – An Evaluation Study

B. R. Srinivas Murthy[1*], Prasanna Raju Yelavarthi[1], N. Devanna[2] and D. Jamal Basha[1]

[1]Pharmaceutics Division, Sri Padmavathi School of Pharmacy, Tirupati, 517503, India.
[2]Oil Technological and Pharmaceutical Research Institute (OTPRI), Jawaharlal Nehru Technological University Anantapur (JNTUA), Ananthapuramu-515002, India.

Authors' contributions

The conception, design, interpretation of results of the study work was carried out in collaboration among all authors. The corresponding author drafted the manuscript and amalgamated the suggestions from co- authors. All authors revised and approved the final manuscript.

Article Information

DOI: 10.9734/JPRI/2021/v33i1831316
Editor(s):
(1) Dr. Mohamed Salem Nasr Allah, Weill Cornell Medical College, Qatar.
Reviewers:
(1) María Esperanza Ruiz, Laboratorio de Investigación y Desarrollo de Bioactivos (LIDeB), Universidad Nacional de La Plata, Argentina.
(2) Gabriela Garrastazu Pereira, Lisbon University, Portugal.
Complete Peer review History: http://www.sdiarticle4.com/review-history/66721

Original Research Article

Received 20 January 2021
Accepted 24 March 2021
Published 29 March 2021

ABSTRACT

Aim: Guggul lipid, a lipophillic antihyperlipidemic moiety, undergoes extensive first-pass metabolism and has low bioavailability. In order to address this limitation, guggul lipid loaded chitosan nanoparticles (GNPs) were designed, optimized and processed by 3- factor 3- level Box-Behnken design (BBD).
Methodology: A 3-factor 3-level BBD was employed to investigate combined influence of formulation variables on percent entrapment efficiency (EE) and percent drug release (DR) of GNPs prepared by ionic gelation method. The generated polynomial equation was validated and desirability function was utilized for optimization. Optimized GNPs were evaluated for physicochemical, morphological, release characteristics, solid state characterization and in-vitro cell line studies.
Results: Amounts of chitosan, sodium tripolyphosphate and guggul were selected as independent variables had variably influenced EE and DR. Optimized GNPs were produced with an average

**Corresponding author: E-mail: seenu46@gmail.com;*

size of 96.5 nm, electro kinetic potential of -15.4 mV, EE of 92.98% and DR of 95.12% in 24 h with sustained release. Physicochemical and in-vitro characterization revealed existence of guggul in amorphous form in GNPs without interaction and exhibited sustained release profile following first order with Higuchi kinetics. GNPs possessed lipase inhibition activity with IC_{50} value of 14.72 µg/ml and better viability against various cell lines with CTC_{50} values (256.24 to 321.27 µg/ml).
Conclusions: Design and optimization of GNPs by BBD proved to be an effective and promising approach. High entrapment of guggul followed controlled release were the outcomes of GNPs prepared by ionic gelation with improved cell viability.

Keywords: Box–Behnken design; chitosan; guggul lipid; hyperlipidemia; ionic gelation; response surface.

1. INTRODUCTION

Hyperlipidaemia is a heterogeneous disorder characterized by increased flux of free fatty acids raised triglycerides (TGs), low-density lipoprotein-cholesterol (LDL) and apolipoprotein B (apoB) levels. Reduced plasma high-density lipoprotein (HDL) cholesterol is due to metabolic effects or dietary and lifestyle habits [1]. Consumption of high fat diet (intake of fat and cholesterol exceeding 40% of total calories uptake), junk food and changes in lifestyle habits are the main reasons behind increasing prevalence of hyperlipidemia and associated disorders [2]. Hyperlipidemia, in turn, may lead to diabetes mellitus, fatty liver, cerebral infarction, hemiplegia and various cardiovascular disorders (CVDs) that accounts for one third of total deaths worldwide by 2020 [3-5].

Several synthetic moieties such as statins, fibrates, bile acid sequesterants, nicotinic acid derivatives, cholesterol absorption inhibitors and lipase inhibitors are prescribed to treat hyperlipidemia widely. However, the therapeutic efficacy of some of the above agents is limited by serious side effects viz., myopathy, rhabdomyolysis, hepatic toxicity, cardiomyopathy, kidney damage, bloating, flatulence, skin rashes, gallstones, abdominal pain, oily spots, diarrhoea and even death. Additionally, novel potential targets like inhibitors of Acyl-CoA cholesterol acyl transferase (ACAT), microsomal triglyceride transfer protein (MTP), cholesteryl ester transfer protein (CETP) and squalene synthase have also been explored but not yet succeeded [6,7]. Thus, the demand to focus on developing multifunctional natural bioactive compounds such as allicin, guggul, citrus flavonoids, curcumin, green tea, epigallocatechin gallate, and resveratrol as alternative therapeutic agents for treating hyperlipidemia and obesity is ever-increasing [8]. Among these, Guggulsterone, an active principal constituent of guggulipid obtained from the gum resin of traditional Ayurvedic plant Commiphora mukul (guggulu in Sanskrit) is approved in India as an antihyperlipidemic drug and has been used in Ayurvedic medicine since 600 BC to treat a wide variety of ailments including arthritis, obesity, hyperlipidemia and other lipid disorders. It also possesses antiseptic, anti-rheumatic, antiulcer, anti-cancer and anti-inflammatory properties [9-11]. Recent research indicated that guggulsterones (E & Z) are antagonists of farnesoid X receptor (FXR), which inhibits CYP7A1, the enzyme responsible for biotransformation of cholesterol, and also inhibits bile acid receptor (BAR), nuclear hormone receptors involved in bile acid regulation and cholesterol metabolism there by directly reduces hepatic cholesterol levels in humans [12]. However the antihyperlipidemic efficacy of the above mentioned natural agents depends of the design of suitable delivery systems.

In recent years nanoencapsulation of plant extracts and herbal drugs have revealed numerous advantages like enhanced solubility, bioavailability and therapeutic response, among others [13]. It also may provide protection from chemical degradation, reduced toxicity, targeted delivery and sustained/controlled action [14]. Among different approaches explored so far, colloidal carriers are of particular interest, especially those made from natural polymers [15]. Among biopolymers, chitosan is one of the most promising coating materials for many bioactive agents due to its nontoxic, biocompatible, and biodegradable characteristics [16,17]. In this context, the present research was aimed to design and optimize guggul loaded chitosan nanoparticles (GNPs) by ionic gelation method, optimized by a Box-Behnken Design (BBD), and to improve the release characteristics and antihyperlipidemic potential.

2. MATERIALS

Guggul lipid was procured from M/s. Chemilloids (Vijayawada, India), Chitosan (MW 150 kDa, degree of deacetylation >87%) was purchased from Aura Biotech Pvt ltd (Chennai, India). Sodium tri polyphosphate (TPP) was purchased from Sigma-Aldrich (Bangalore, India). Milli Q water was used throughout the study. Dulbecco's modified eagle's medium (DMEM), fetal bovine serum (FBS), antibiotic-antimycotic mixture, trypsin, dimethyl sulfoxide (DMSO), 3-(4, 5-dimethylthiazol-2-yl)-2, 5-diphenyltetrazolium (MTT) and biochemical assay kits were purchased from Himedia (Mumbai, India). All other chemicals and materials used in the study were of analytical grade.

3. METHODS

3.1 Drug-excipient Compatibility Studies (FTIR)

Compatibility studies for guggul, chitosan, sodium tripoly phosphate (TPP) and GNPs were studied by Fourier Transform Infrared (FTIR) spectroscopy (Shimadzu 8300E). FTIR spectra of guggul, chitosan, TPP and GNPs were studied by KBr pellet method. Each spectrum of the sample was collected from 32 single average scans at a resolution of 4 cm^{-1} in the absorption region of 400-4000 cm^{-1} [18].

3.1.1 Preparation of guggul chitosan nanoparticles

Guggul chitosan nanoparticles (GNPs) were prepared via ionic gelation method. A weighed quantity of chitosan was dissolved in Milli-Q water. Subsequently, a predefined quantity of guggul (dissolved in 0.2 ml of methanol) was added to chitosan solution under stirring. NPs were formed by adding TPP solution at a constant flow rate of 0.5 ml/min under stirring at 600 rpm at room temperature and allowed to crosslink for 3 h. Thereafter, GNP suspension was subjected for ultrasonication (Sonics VC 750) for 15 min, producing nanoparticles with controlled and uniform size. The dispersion was centrifuged at 7500 rpm for 20 min (Remi, Mumbai, India). Sediment was washed, redispersed in 1% lactose as cryoprotectant, lyophilized at -60°C and stored till further use [19,20]. As shown in Table 1, 17 different formulations were prepared.

3.1.2 Box-Behnken Design (3 Factor -3 Level with 5 Center Points)

BBD with statistical model incorporating interactive and polynomial terms were utilized to optimize and assess the responses. In this study, BBD with three factors at three levels were employed to generate quadratic response surface and second order polynomial models to quantify and thereby to optimize the GNPs. Based on preliminary studies, amounts of chitosan (X_1), TPP (X_2) and drug (X_3) were selected as independent variables and evaluated at three different levels: high, medium and low. The percent entrapment efficiency (Y_1) and percent drug release at 24h (Y_2) selected as responses with applied constraints are described in Table 2. Seventeen runs were generated using the Design Expert 8.0.6 software (State Ease, Inc., Minneapolis, MN). All experiments were performed in randomized manner to eradicate possible sources of bias. The non-linear quadratic model generated by the BBD was:

$$Y = A_0+A_1X_1 +A_2X_2 +A_3X_3 +A_4X_1X_2 +A_5X_2X_3 +A_6X_1X_3 +A_7X_1^2 +A_8X_2^2 +A_9X_2^3+ E \quad (1)$$

Where Y is the measured response associated with each factor-level combination; A_0 is an intercept; A_1–A_9 are the regression coefficients; A_1–A_3 are main effects of X_1–X_3; A4-A9 are effects of main factors and E is error term.

Multiple linear regressions and ANOVA were carried out for deciding the significance and influence of each individual factor as well as their interactions on response variables. A checkpoint analysis was performed to confirm the role of the derived polynomial equation and contour plots in predicting the responses. Optimization was performed by the desirability approach [21,22].

3.2 Evaluation of GNP

3.2.1 Entrapment efficiency (EE)

The amount of guggul entrapped in the GNPs was assessed by an indirect method. Before lyophillization, the nanoparticle suspension was centrifuged at 7500 rpm for 20 min. The clear supernatant was collected, filtered through a membrane filtered disc (0.22 µm) and guggul quantification was performed in an UV spectrophotometer (brand, city) at 254 nm. The EE was calculated according to the following expression:

$$\text{EE}\ (\%) = \frac{W_t - W_s}{W_t} \times 100 \quad (2)$$

Where W_t represents the total amount of guggul used for the preparation of nanoparticles and W_s represents the amount of free guggul in supernatant liquid [23].

3.3 *In-vitro* Drug Release Study

The *in vitro* release profile of guggul from the GNPs was determined using dialysis tubing. Nanoparticles equivalent to 50 mg of guggul were placed in a dialysis bag (MWCO 12,000–14,000 g/mol, pore size of 2.4 nm). The dialysis bags were tied USP apparatus 2 (paddle) and suspended in dissolution vessels containing 500 ml of PBS pH 7.4. Aliquots of 5 ml were withdrawn at 0.5, 1, 2, 3, 4, 6, 8, 12 and 24 h by maintaining sink condition. Further, samples were filtered through a 0.22 µm membrane filter and analysed by UV spectrophotometry (Shimadzu UV-1800) at 254 nm. Three replicates of each experiment were carried out and the cumulative percentage of drug release was calculated. Data obtained from the *in vitro* release studies were fitted to various kinetic models [24].

3.3.1 Identification of optimum formulation

Numerical optimization technique was adapted for optimizing the formulation variables to obtain desired responses. The (predicted) optimum formulations were prepared in triplicate in order to asses the accuracy of the prediction. Mean values of experimental data were compared against predicted values and percent error was determined. Data obtained were screened to assess the accuracy and suitability of the conditions employed in the preparation of GNPs.

3.4 Characterization of Optimized Formulation

3.4.1 Particle size, Zeta potential and morphology

Particle size distribution and zeta potential of GNPs (optimized formulation) were estimated using Zetasizer (Horiba SZ-100). Measurements were performed by dynamic light scattering technique with scattering angle of 90° at 25 ± 0.5°C. [16] Morphology of optimized GNPs was analysed by high resolution scanning electron microscope (Carl Zeiss Merlin Compact, Chennai). For that, the GNPs sample was placed on an aluminium stub, dried under vacuum and then sputtered with gold. Coated samples were placed in vacuum and the images were captured at an acceleration voltage of 3 kV [25,26].

3.5 Differential Scanning Calorimetry

Chemical compatibility of guggul with formulation components and its physical state in GNPs was assessed by differential scanning calorimetry (DSC-60, Shimadzu). Each sample was loaded on an aluminium pan followed by heating through nitrogen (flow 30 ml/min) at scanning rate of 5°C/min from 25 to 200°C. Same quantity of indium was used as a reference in aluminium pan, and the heat flow as a function of temperature was measured [21,27].

3.6 X-ray Diffraction Study

The X-ray diffraction (XRD) pattern was recorded for guggul, chitosan and GNPs using an X-ray diffractometer (Horizon, Chennai) at room temperature, with a voltage of 30 kV, 5 mA current and a 4°/min scanning speed. The samples were scanned from 5 to 50° (2θ) with a step size 0.01° and a step interval of 0.1 sec [28].

3.7 *In-vitro* Cell Line Studies

3.7.1 Cell culture and stimulation

3T3-L1 mouse fibroblasts, NSC-34 (mice motor neuron like) and kidney epithelial cells (Vero cells) were obtained from the National centre for cell sciences (Pune, India). Cells were cultured in dulbecco's modified eagle's medium (DMEM) with 10% (v/v) bovine calf serum (BCS) and 1% (v/v) penicillin-streptomycin. Two days after confluence, the cells were stimulated to differentiate with DMEM containing 10% fetal bovine serum (FBS), 0.5 mM 3-isobutyl-1-methylxanthine (IBMX) and insulin (10 µg/ml) for two days. Cells were then maintained in 10% DMEM/ FBS medium with insulin (10 µg/ml) for another two days followed by culturing with a 10% FBS/DMEM medium for an additional four days, where >90% of cells were differentiated 3T3-L1 adipocytes with lipid droplets accumulated. Differentiated 3T3-L1, NSC-34 and Vero cells were then treated with GNPs. The cells were maintained at 37ºC with 5% CO_2 throughout the experiments.

3.7.2 Cell viability – MTT assay

Cells were grown and seeded at a density of 1 × 10^4 cells/well in 96 well plates. Cells were then

treated with GNPs and incubated with 3-(4, 5-dimethylthiazol-2-yl)-2, 5-diphenyltetrazolium (MTT) solution for 3 h at 37ºC. Supernatants were aspirated, DMSO was added to each well, and then plates were agitated to dissolve the crystal product. Absorbance was measured at 540 nm using a microplate reader (Tecan M200). All experiments were performed in triplicate and mean values were used for calculation of circulating tumor cells (CTC_{50}) as per the following equation

$$\%\text{Viability} = \frac{\text{Absorbance of the test sample}}{\text{Absorbance of the control}} \times 100 \quad (3)$$

All experiments were performed in triplicate and mean values were used for calculation of CTC_{50} [29,30].

3.8 Lipase Inhibition Studies

In-vitro lipase inhibition of optimized GNPs were performed as per the standard procedures [30].

3.8.1 Lipase suspension

Lipase powder was suspended in a Tris buffer pH 8.4 at a concentration of 5 mg/ml, the suspension was centrifuged and the supernatant was used for enzymatic reaction.

3.8.2 Sample preparation for lipase inhibition assay

Samples of GNPs for lipase inhibition were taken during the dissolution studies. Aliquots (5 ml) taken at specified time intervals were centrifuged at 10,000 rpm for 5 min, the supernatants were filtered and used for the assay.

3.8.3 Methods

In vitro assay of lipase activity was analyzed according to Lee et al. (1993). Enzyme assays were performed in 96-well microplate by adding 78 µl of GNP dissolution sample. After 20 min pre-incubation of inhibitor with lipase in the presence of bile salts, 100 µl of substrate p-nitro phenyl butyrate (p-NPP) were added and the absorbance was measured immediately at 410 nm using a microplate reader. Extent of lipase inhibition of GNPs was compared with guggul [31].

3.9 Stability Studies

Stability studies of optimized GNPs were carried out at room temperature (25±2°C), refrigerated condition (4±1°C) and accelerated condition (40±2°C/75±5%RH) over a period of three months. Samples were evaluated at 0, 30, 60 and 90th day by FTIR, drug content and drug release as indicators for physicochemical intactness [22].

3.10 Statistical Analysis

All experiments were performed in triplicate. The results were given as mean ± standard deviation (SD). Statistical comparisons of data were made with simple analysis of variance (ANOVA) and independent student t-tests. The level of significance was taken as $p<0.05$.

4. RESULTS

4.1 Experimental Design

In experimental design, the effect of independent variables, i.e. amounts of chitosan (X_1), TPP (X_2) and guggul (X_3) on dependent variables such as % EE (Y_1) and % DR (Y_2) of 17 formulations was studied and results are depicted in Table 1.

4.2 Effect on % Entrapment Efficiency

The %EE of GNPs was ranged between 83.1±0.05% to 96± 0.13% (Table 1). The polynomial equation showing the effect of independent variables was obtained as

$$Y_1 = 94.87 + 2.44\ X_1 + 0.92X_2 + 2.59X_3 + 0.15X_1X_2 + 2.44X_1X_3 - 2.22\ X_2X_3 - 0.52X_1^2 - 0.78\ X_2^2 - 3.53X_3^2 \quad (4)$$

The quadratic model had p values (global) of <0.0001 and F ratio of 58.57 stated that the model was significant for EE. The R^2 value of 0.986 for polynomial equation also indicated a good fit. Hence, this model was used to navigate the design space. All the independent variables X_1, X_2 and X_3 and their interactive effects significantly affected % EE as shown in Fig. 1.

4.3 Effect on % Drug Release

Drug release from GNPs at 24 h varied at the range of 88.56±0.86% to 96.12±0.42% up to 24 h as consequence of change in independent variables (Table 1 and Fig. 2). The polynomial equation showing the effect of independent variables on DR was as followed:

$$Y_2 = 95.50 + 1.72X_1 + 0.30X_2 + 1.10\ X_3 - 0.32\ X_1X_2 + 0.26X_1X_3 - 1.64\ X_2X_3 - 0.03X_1^2 - 1.13\ X_2^2 - 2.83X_3^2 \quad (5)$$

Table 1. BBD matrix with three independent variables at three levels and observed responses

	Factor 1	Factor 2	Factor 3	Response 1	Response 2
Run	A:Polymer (mg)	B:Crosslinker (mg)	C:Drug (mg)	EE (%)	DR (%)
1	2000	2250	200	92.86 ±0.61	92.89±0.20
2	1500	1500	350	90.57±0.08	91.93±0.34
3	1750	1500	200	84.83±0.59	88.56±0.86
4	1750	2250	350	95.18±0.54	95.49±0.49
5	1750	3000	500	91.83±0.85	91.23±0.50
6	1750	2250	350	95.89±0.79	95.97±1.17
7	1500	2250	500	93.62±0.31	91.86±0.62
8	1500	3000	350	91.68±0.43	93.19±0.74
9	1750	2250	350	94.08±0.15	95.37±0.35
10	1750	3000	200	91.56±0.07	92.44±1.11
11	1750	2250	350	94.76±0.88	95.67±0.74
12	1500	2250	200	83.1±0.05	90.08±0.62
13	2000	1500	350	95.12±0.21	96.12±0.42
14	1750	2250	350	94.43±0.54	94.98±1.02
15	1750	1500	500	93.97±0.24	93.92±0.68
16	2000	2250	500	93.64±0.66	95.72±0.64
17	2000	3000	350	96.84±0.13	96.08±0.46

All data are shown as mean ± S.D; n=6

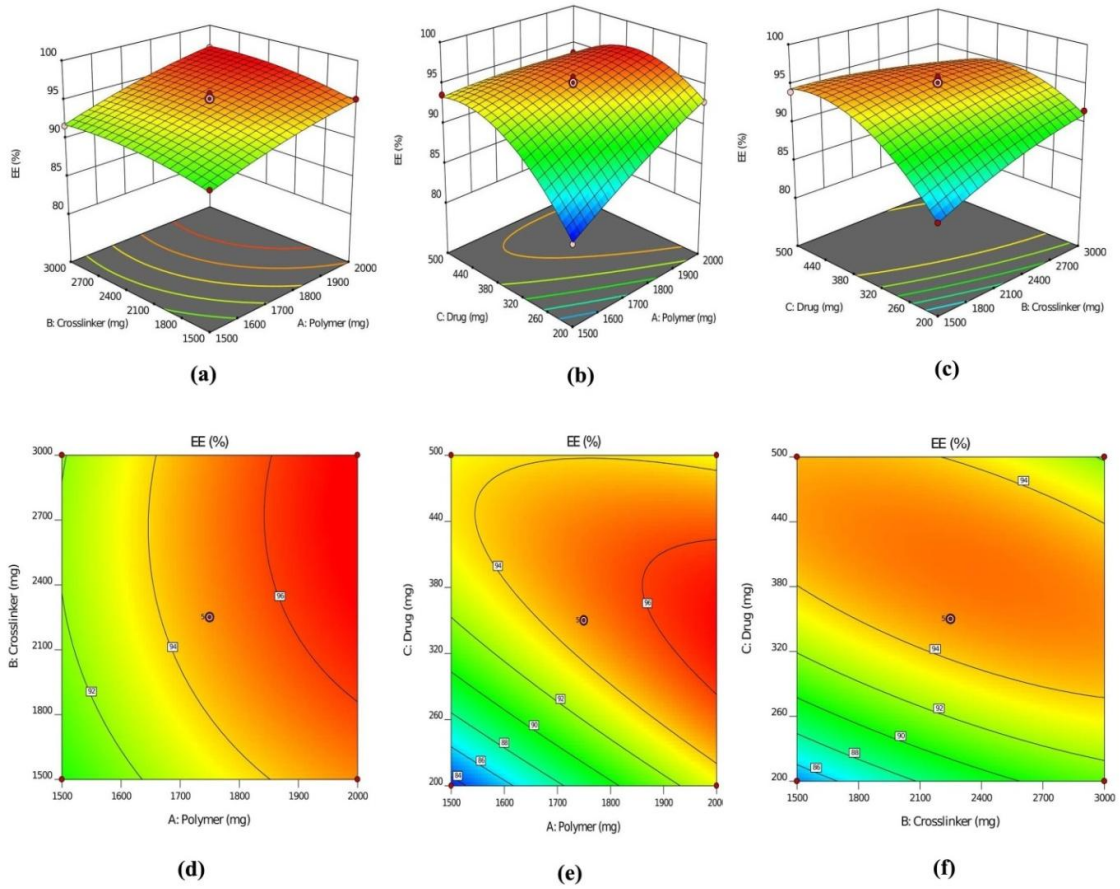

Fig. 1. 3D response surface (upper line) and contour (bottom line) plots of EE as a function of: (a) and (d) chitosan and TPP amounts; (b) and (e) chitosan and guggul amounts, and; (c) and (f) TPP and guggul amounts

Table 2. Formulation variables in BBD used to prepare 17 formulations

Factors	Coded levels of variables		
	Low (-1)	Medium (0)	High (+1)
Independent variables			
X_1= Chitosan (mg)	1500	1750	2000
X_2= Sod. TPP (mg)	1500	2250	3000
X_3= Guggul lipid (mg)	200	350	500
Dependent variables (Responses)			
Y_1= % Entrapment Efficiency (%EE)		Maximize	
Y_2= % Drug Release (%DR at 24h)		Maximize	

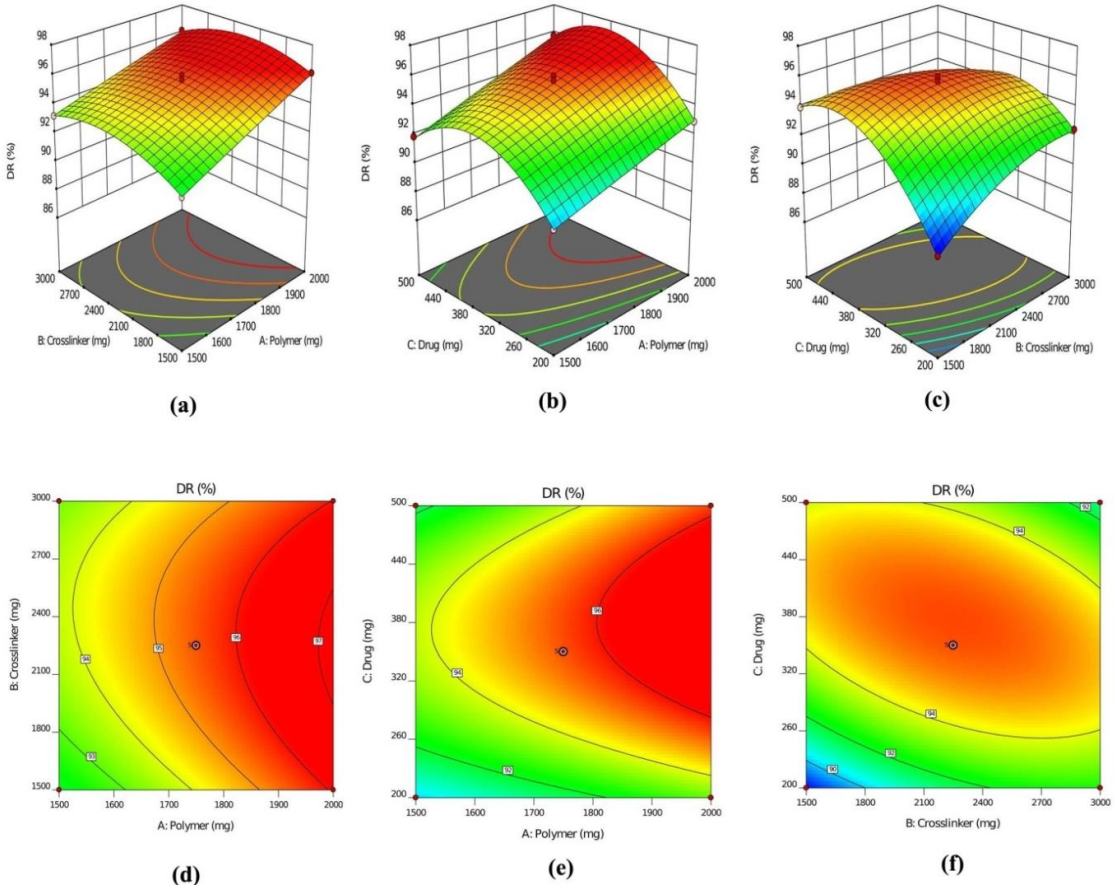

Fig. 2. 3D response surface (upper line) and contour (bottom line) plots of DR as a function of: (a) and (d) chitosan and TPP amounts; (b) and (e) chitosan and guggul amounts, and; (c) and (f) TPP and guggul amounts

Quadratic model had p values of <0.0001 and F value of 114.75, implying that the model was significant for DR. Predicted and experimental values were justified by correlation coefficient (R^2) which was found to be 0.9933 and indicated a good fit.

Response surface plots elucidated the effect of independent variables (X_1, X_2 and X_3) on drug release. The drug release profiles of the different formulations are depicted in Fig. 3. For both dependent variables, parity plots (Fig. 4a and 4b) show strong agreement between experimentally measured responses and the ones predicted by the models. Correlation coefficients demonstrated good relationship between the observed values and the responses predicted by the models. Normal (percentage) probability

plots (Fig. 4c and 4d) demonstrated that errors were normally distributed, and were independent of each other with homogenous error variance. Residual plots (Fig. 4e and 4f) showed that higher predicted values are associated with higher variance. These data further confirmed the reliability of the quadratic models.

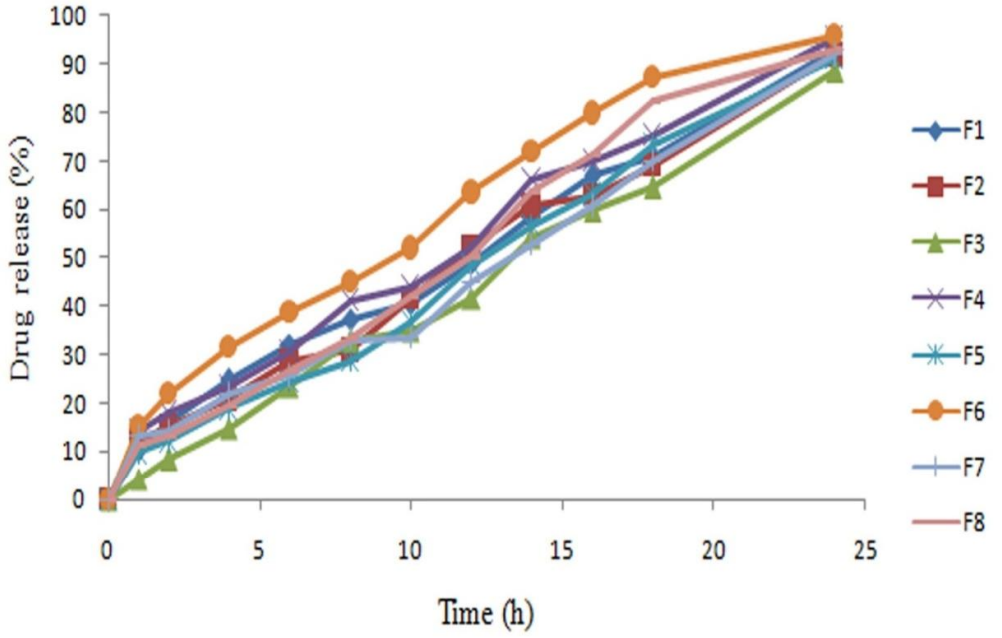

(a)

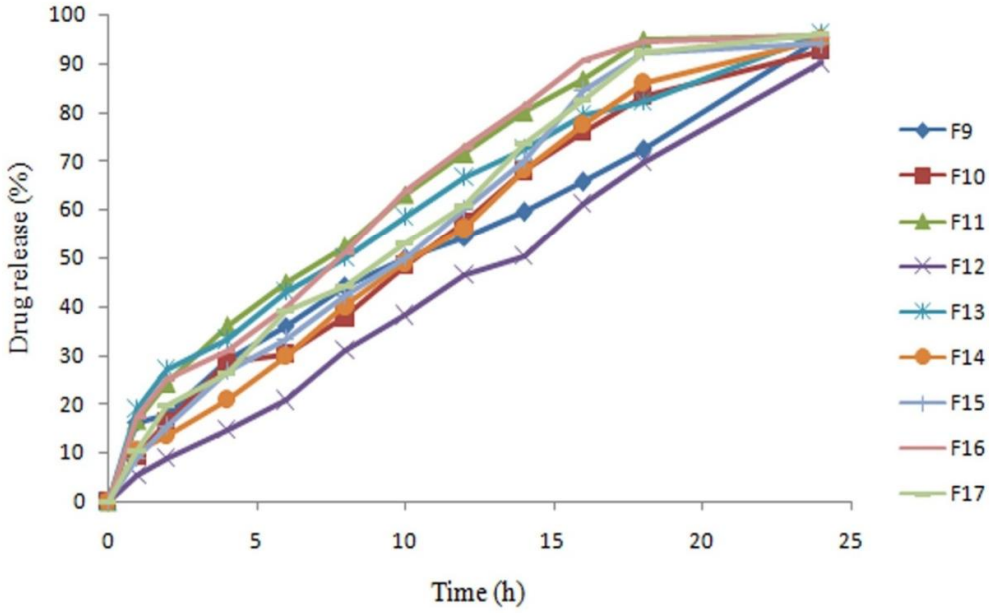

(b)

Fig. 3. Drug release profiles of GNPs F1-F17

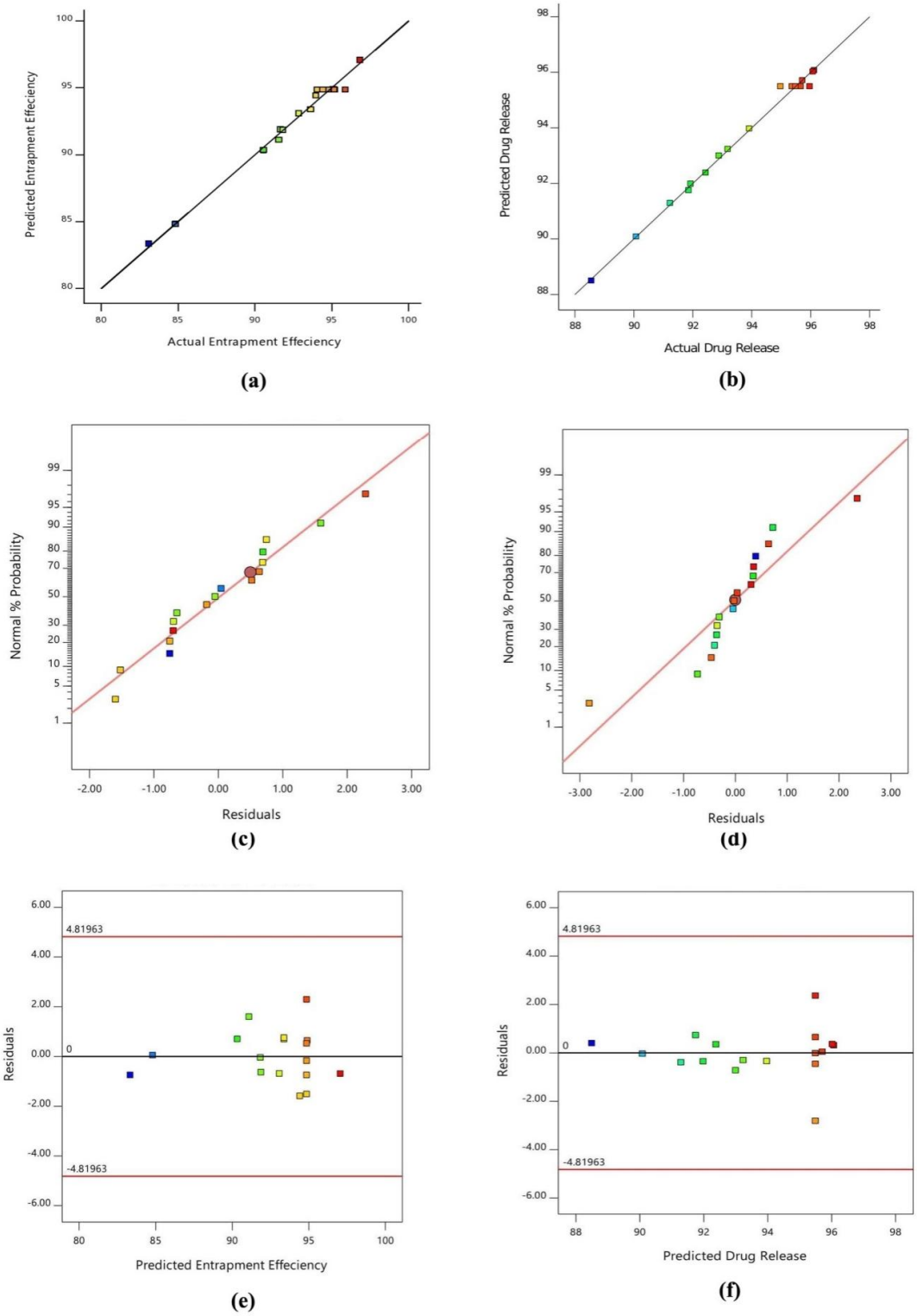

Fig. 4. Parity charts of predicted versus observed responses for (a) EE and (b) DR. Normal (percentage) probability of residuals for (c) EE and (d) DR. Residual plot of (e) EE and (f) DR

4.3.1 Optimization using desirability approach

Numerical optimization technique based on the desirability approach was employed for optimization of GNPs to achieve maximum entrapment efficiency and desired drug release. Levels of variables (X_1, X_2 and X_3) that produced optimum responses were found to be 1733.94, 1833.97 and 342.69 mg, respectively, with predicted 94.86 ± 0.24% EE and 95.49 ± 0.68% DR and overall desirability of 1. Optimized GNPs yielded EE of 92.98 ± 0.47% and DR of 95.12 ± 0.36% which were very close to predicted values with low percentage of bias. The % yield of optimized GNPs was found to be 85.84%.

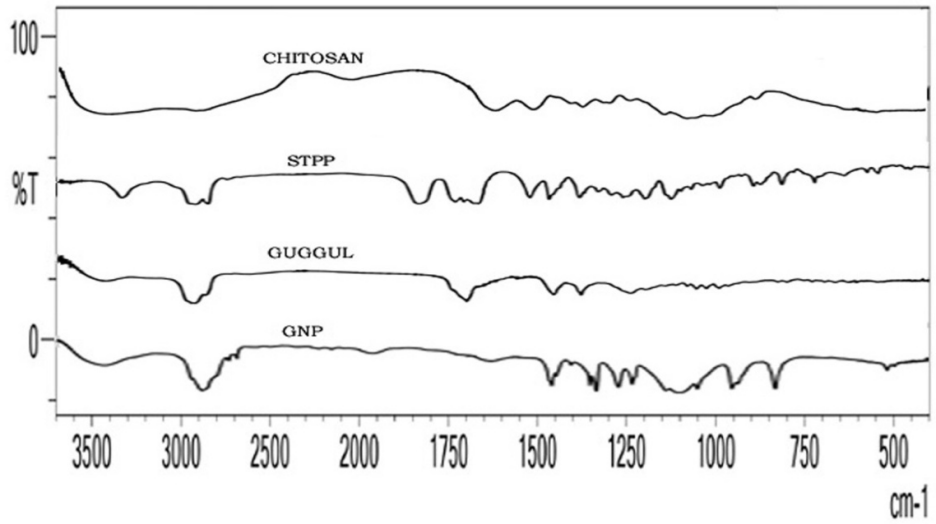

(a)

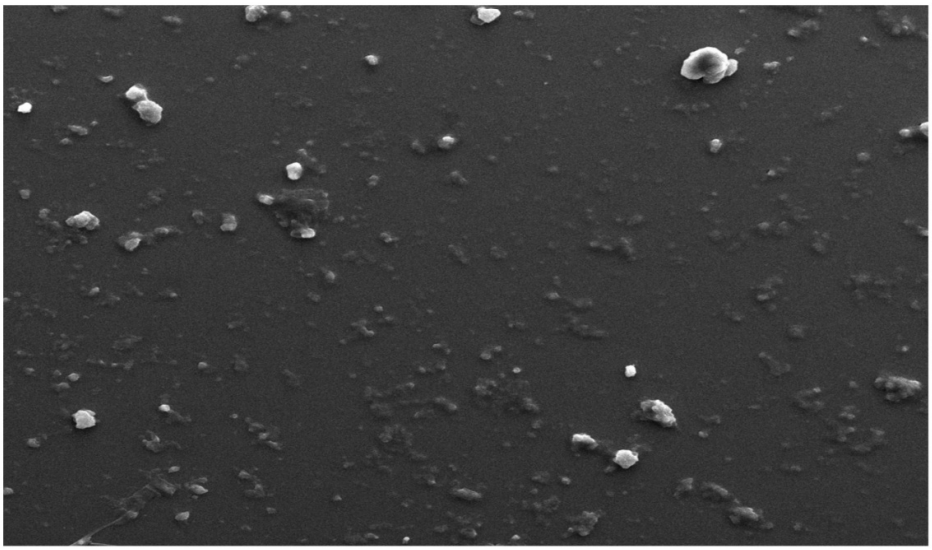

(b)

Fig. 5. (a) FTIR spectra of Chitosan, TPP, guggul and GNP and (b) SEM of GNPs

4.4 Characterization of Optimized GNPs

4.4.1 FTIR spectroscopy

FTIR spectrum of guggul (Fig. 5a) had major characteristic absorption peaks at 1700.78 cm^{-1} (C=O stretching), 1455.05 cm^{-1} (C=C aromatic stretching), 2869.39 cm^{-1} (CH stretching), 3443.70 cm^{-1} (combined peaks of $-NH_2$ and -OH) 2955.18 cm^{-1} (C-H vibration), 1737.58 cm^{-1} (C=O stretching), 1671.98 cm^{-1} (C=C stretching), 1409.31 cm^{-1} (CH_2 bending), 1383.07, 1340.77 and 1260.96 cm^{-1} (O-H bending), 1095.11 and 1026.82 cm^{-1} (C-F bending), 1169.51 cm^{-1} (C-0 stretch), 884.52 cm^{-1} due to distribution of aromatic protons and 759 cm^{-1} due to CH_2 rocking respectively. FTIR spectrum of chitosan showed characteristic peak at 1515.77 (CH stretching), 1628.63 cm^{-1} (C=O stretching of amide I), 1700.78 cm^{-1} (C=O), 3421 cm^{-1} (combined peaks of primary $-NH_2$ and -OH). FTIR of TPP showed a characteristic peak at 2915 cm^{-1} (C-H stretching). Most characteristic peaks of guggul and chitosan were retained in spectrum of GNPs, indicating no interaction between integrants.

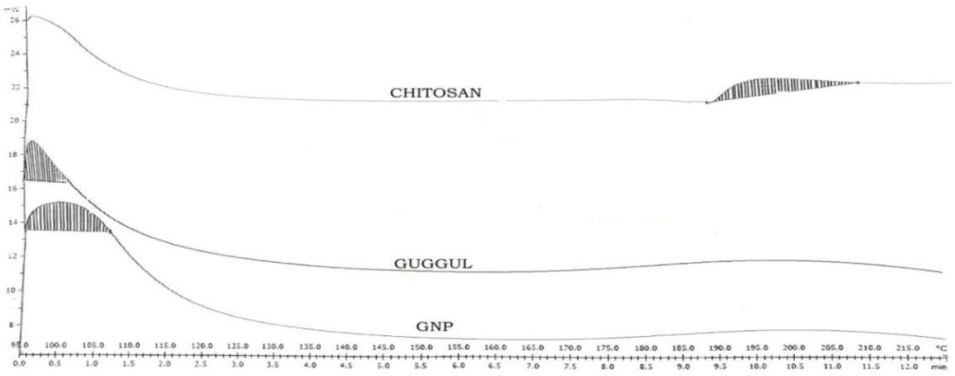

(a)

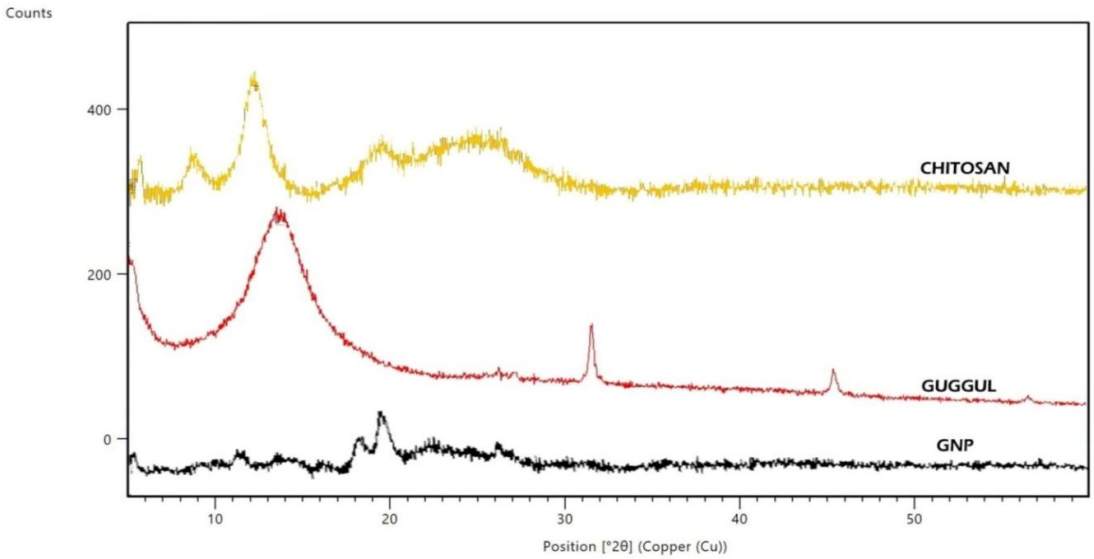

(b)

Fig. 6. (a) DSC thermograms of GNPs and (b) XRD of GNPs

4.5 Particle Size, Zeta Potential and Morphology

Particle size and zeta potential of optimized GNPs were 96.5 nm and -15.4 mV, respectively. Optimized GNPs were found to be spherical, uniformly distributed with slight rough and porous texture (Fig. 5b).

4.6 Differential Scanning Calorimetry

Thermograms of chitosan, guggul and GNPs are depicted in Fig. 6a. An endothermic peak of guggul is observed at 92.89°C, retained in thermogram of GNPs.

4.7 X-ray Diffraction

XRD of guggul (Fig. 6b) showed a range of sharp peaks at 2θ values from 10.0 to 45.0. Some of the peaks of guggul were disappeared in GNP stating slight amorphization.

4.8 Stability Studies

Stability studies data revealed that there were no physicochemical changes of GNPs and no shift in the principal functional groups of guggul as noticed in FTIR spectra (Data not shown). There was no significant difference between the samples stored at stressed conditions in terms of physicochemical integrity, drug content (91.36%) and drug release (89.84-95.12%) of optimized formulation. The developed GNPs were found to be physicochemically stable over a period of three months. The release of guggul from GNP followed First-order with Higuchi kinetics up to 24 h.

4.9 *In vitro* Cell Line Study (MTT Assay)

Optimized GNPs showed better level of cell viability against the three selected cell lines. For 3T3-L1 mouse fibroblasts, NSC-34 (mice motor neuron like) and kidney epithelial cells (Vero cells) the function of cell viability i.e., CTC_{50} values of GNPs were found to be 270.72, 256.24 and 321.27 µg/ml and that of pure guggul was 310.63, 297.76 and 375.87 µg/ml, respectively.

4.10 Lipase Inhibition

IC_{50} values of GNPs and guggul were found to be 14.72 and 20.63 µg/ml, respectively, indicating good inhibition of lipase enzyme.

5. DISCUSSION

Design and optimization of formulation by using Box Behnken experimental Design (BBD) was a good conceptual approach. BBD depicted the effect of dependent variables on independent variables in a well-designed experiment with lowest number of runs in a systematic manner. BBD also allowed the establishment of optimal parameters by suitable mathematical and graphical representation. Coefficients (A_1, A_2 and A_3 of equation (1)) with one factor in quadratic polynomial equations were attributed to main effect (EE or DR) of that particular factor, while coefficients with more than one factor were attributed to interaction between those variants. A positive coefficient factor indicated direct relationship between factor and response, whereas negative coefficient indicated converse effect. Response surface graphs were generated using polynomial equations, which represented simultaneous effect of two variables on response parameters by taking one variable at a constant level. Increased EE with increased chitosan (X_1) could be attributed to more amount of chitosan that had higher ability to form ionic gel with increased viscosity of dispersion thereby increased diffusional resistance of guggul to move forward into external phase through polymer droplet [16]. Moreover, time required for polymer precipitation decreased at higher polymer concentration and rapidly precipitated on the surface of dispersed phase, which prevented guggul molecules to diffuse out of GNPs across the phase boundary. Increased EE with corresponding increase in TPP (X_2) might be due to better crosslinking of chitosan matrix and more chitosan molecules could be participated in ionic gelation process which reconciled more guggul. Guggul (X_3) had direct correlation with EE where, more number of guggul molecules/micronized particles interacted with chitosan through electrostatic forces, thereby high proportion of guggul was entrapped in GNPs. Interaction factors X_1X_2 and X_1X_3 (equation (4)) were positively related to the EE owing to the above phenomena. However, the reason behind contrary relation of X_2X_3 with EE was not clear, but might be due to anionic nature of both TPP and guggul that competitively interacted with similar chemical group of chitosan, thereby affecting the cross-linking efficiency.

Drug release was significantly The curvilinear increase in drug release with increased TPP (X_2, see Fig. 2) could be due to effective cross linking with hydrophilic polymer, where more

polyphosphoric ions cross-linked with amino groups on chitosan chains that loaded more guggul within its network and sustained its release from the NPs. Similarly, guggul (X_3) showed significant positive effect on drug release where higher amount of guggul resulted in greater entrapment with better release.

As check point analysis, there was an excellent agreement between responses measured and predicted for EE and DR. Experimental values were very close to predicted values, with low percentage bias, hence suggested that the employed mathematical model was reliable. Consequently, numerical optimization technique was employed for optimization of GNPs. Optimal concentrations of chitosan, TPP and guggul (1733.94 mg, 1833.97 mg and 342.69 mg respectively) produced a promising nanoformulation with EE of 92.98% and DR of 95.12% and overall desirability of 1.

GNPs were prepared by ionic gelation technique wherein, positively charged primary amine groups of chitosan interacted with negatively charged groups of polyanion (TPP). Further TPP, being a crosslinker with multivalent characteristics, helps in maintaining the chemical integrity of both chitosan and guggul in GNPs, which was evident from FTIR spectra. However, a peak at 1740 cm^{-1} and 1700.78 cm^{-1} of guggul and chitosan disappeared in the GNPs, due to linkage between phosphoric groups of guggul, TPP and ammonium groups of chitosan. Cross-linked GNPs also showed a peak at 1060.75 cm^{-1} (P=O) and broader peak between 2941–3443 cm^{-1} owing to hydrogen bonding between -OH and -NH_2 groups. Moreover, all the characteristic peaks of guggul were retained in GNPs and indicated successful encapsulation of guggul in NPs without any modification. Optimized GNPs were found to be stable with intended particle size, drug content, expected drug release and sufficient electrostatic repulsion with slightly negative electrokinetic potential (-15.4 mV) due to excess TPP ions.

Guggul-loaded nanosized (96.5 nm) entities initially released drug in burst mode owing to weak bonding of drug on huge surface of chitosan nanoparticles and later entangled guggul was released out in controlled mode following First order kinetics of Higuchi model up to 24 h. In addition to this biphasic drug release, chitosan-based nanoparticles can interact with negatively charged mucosal surfaces, resulting in enhanced drug absorption and bioavailability because of much longer residence time in gastrointestinal tract which in turn results in reduction of dosing frequency and hence patient compliance is expected to improve.

An endothermic peak of guggul was retained in thermogram of GNPs inferred that there was no physical and phase transition of drug in the mixture of formulation integrants. Similarly in X-ray diffractograms, characteristic peaks of guggul were reduced due to amorphous dilution. Thus, indicated both physical/chemical integrity of stable nanoparticles with promised ionic gelation technique. These stable GNPs were intact against different stress conditions over three months as evident with FTIR spectral elucidation. The optimized GNPs were compatible against 3T3-L1 mouse fibroblasts, mice motor neuron like and Vero cells as evidenced with CTC_{50} values. However, these GNPs did not influenced reduction of MTT and hence above cells were viable against them.

Optimized GNPs hydrolyzed the chromogenic ester of lipase effectively as assessed the yellow coloured p-nitrophenol product and thus indicating the viability of GNPs with the cells. Lipase inhibition activity of GNPs will be an additive effect in treating hyperlipidemia/obesity. Therefore, as the optimized GNPs maximized in vitro attributes of drug delivery system such as entrapment, controlled drug release, cell viability, lipase inhibition and physicochemical inertness, these formulations are appropriate delivery systems, with the potential to target the fat and adipose tissues in the treatment of obesity and hyperlipidemia.

6. CONCLUSION

Guggul loaded chitosan nanoparticles were successfully prepared by ionic gelation and optimized by a 3-factor 3-level BBD. The optimized formulation released guggul over a period of 24 h by following Higuchi kinetics. The optimized GNPs witnessed controlled release with better cell viability, additional lipase inhibition activity and were physicochemically intact against stress conditions over a period of 3 months. Thus, guggul loaded nanoparticles produced by ionic gelation proved as a better alternative to conventional dosage forms provided their high entrapment efficiency, improved drug release, enhanced lipase activity and high compatibility for various cell lines. Therefore, GNPs can be employed as suitable drug delivery platforms for delivering guggul lipid,

a natural bioactive compound. Further in vivo and preclinical studies using suitable models are essential to prove the antihyperlipidemic potentials of GNPs.

DISCLAIMER

The products used for this research are commonly and predominantly use products in our area of research and country. There is absolutely no conflict of interest between the authors and producers of the products because we do not intend to use these products as an avenue for any litigation but for the advancement of knowledge. Also, the research was not funded by the producing company rather it was funded by personal efforts of the authors.

ACKNOWLEDGEMENTS

The authors are grateful to Sri Padmavathi School of Pharmacy, Tirupati, India for rendering generous support to carry out the research work.

COMPETING INTERESTS

Authors have declared that no competing interests exist.

REFERENCES

1. Badole SL, Farid Menaa F. Therapeutic approaches to drug targets in hyperlipidemia. Bio Med. 2012;2:137-146.
2. Blackburn GL, Wollner S, Heymsfield SB. Lifestyle interventions for the treatment of class III obesity: A primary target for nutrition medicine in the obesity epidemic. Am J Clin Nutr. 2010;91(1):289-292.
3. Lee H, Choi JM, Cho JY, Kim TE, et al. Regulation of endogenic metabolites by rosuvastatin in hyperlipidemia patients: An integration of metabolomics and lipidomics. Chem Phys Lipids. 2018;214:69-83.
4. Guaraldi F, Deon V, Del Bo C, Vendrame S, et al. Effect of short-term hazelnut consumption on DNA damage and oxidized LDL in children and adolescents with primary hyperlipidemia: A randomized controlled trial. J Nutr Biochem. 2018;57: 206-211.
5. Chen YL, Chuan-Hao Xiao. Dynamic lipid profile of hyperlipidemia mice. J Chromatography. 2017;15:165-171.
6. Zhang Y, Wang Z, Jin G, Yang X, Zhou H. Regulating dyslipidemia effect of polysaccharides from *Pleurotus ostreatus* on fat-emulsion-induced hyperlipidemia rats. Int J Biol Macromol. 2017;101:107-116.
7. Shattat GF. A review article on hyperlipidemia: Types, treatments and new drug targets. Biomed Pharmacol J. 2014;7(2):399-409.
8. Rupasinghe HP, Sekhon-Loodu S, Mantso T, Panayiotidis MI. Phytochemicals in regulating fatty acid β-oxidation: Potential underlying mechanisms and their involvement in obesity and weight loss. Pharmacol Ther. 2016;165:153-163.
9. Sinal CJ, Gonzalez FJ. Guggulsterone: An old approach to a new problem. Trends in Endocrine Met. 2002;13(7):275–276.
10. Deng R. Therapeutic effects of guggul and its constituent guggulsterone: Cardiovascular benefits. Cardiovasc Drug Rev. 2007;25(4):375-390.
11. Shields KM, Moranville MP. Guggul for hypercholesterolemia. Am J Health Syst Pharm. 2005;62(10):1012-1014.
12. Urizar NL, Moore DD. Gugulipid: A natural cholesterol-lowering agent. Ann Rev Nut. 2003;23:303–313.
13. Prabaharan M, Mano JF. Chitosan-based particles as controlled drug delivery systems. Drug Del. 2005;12(1):41-57.
14. Ajazuddin, Saraf S. Applications of novel drug delivery system for herbal formulations. Fitoterapia. 2010;81(7):680-689.
15. Campos AM, Diebold Y, Carvalho EL, Sanchez A, Alonso MJ. Chitosan nanoparticles as new ocular drug delivery systems: *In vitro* stability, *in vivo* fate and cellular toxicity. Pharm Res. 2004;21(5): 803-10.
16. Rukmangathen R, Yallamalli IM, Yalavarthi PR. Formulation and biopharmaceutical evaluation of risperidone-loaded chitosan nanoparticles for intranasal delivery. Drug Dev Ind Pharm. 2019;45(8):1342-1350.
17. Agnihotri SA, Mallikarjuna NN, Aminabhavi TM. Recent advances on chitosan-based micro- and nanoparticles in drug delivery. J Contr Rel. 2004;100(1):5-28.
18. Rawal T, Mishra N, Jha A, Bhatt A. Chitosan nanoparticles of gamma-oryzanol: Formulation, optimization and *in vivo* evaluation of anti-hyperlipidemic activity. AAPS PharmSciTech. 2018;19(4): 1894-1907.
19. Servat-Medina L, Gonzalez-Gomez A, et al. Chitosan-tripolyphosphate nanoparticles as *Arrabidaea chica*

standardized extract carrier: Synthesis, characterization, biocompatibility and antiulcerogenic activity. Int J Nanomedicine. 2015;10:3897-909.
20. Da Silva SB, Amorim M, Fonte P, Madureira R, et al. Natural extracts into chitosan nanocarriers for rosmarinic acid drug delivery. Pharm Biol. 2015;53(5):642-652.
21. Katamreddy JD, Yalavarthi PR, Rao DS, et al. *In vitro* characterization of statistically optimized quetiapine- loaded self- nanoemulsified systems with quality by design. Int J Pharm Inv. 2018;8(1):14-23.
22. Gajra B, Patel RR, Dalwadi C. Formulation, optimization and characterization of cationic polymeric nanoparticles of mast cell stabilizing agent using the Box-Behnken experimental design. Drug Dev Ind Pharm. 2016; 42(5):747-757.
23. Honary S, Ebrahimi P, Hadianamrei R. Optimization of particle size and encapsulation efficiency of vancomycin nanoparticles by response surface methodology. Pharm Dev Technol. 2014; 19(8):987-998.
24. Wilson B, Samanta MK, Santhi K. Chitosan nanoparticles as a new delivery system for the anti-Alzheimer drug tacrine. Nanomedicine. 2010;6(1):144-152.
25. Shah HA, Patel RP. Statistical modeling of zaltoprofen loaded biopolymeric nanoparticles: Characterization and anti-inflammatory activity of nanoparticles loaded gel. Int J Pharm Investig. 2015; 5(1):20-27.
26. Zamora-Mora V, Fernandez-Gutierrez M, San Roman J. Magnetic coreshell chitosan nanoparticles: Rheological characterization and hyperthermia application. Carbohydr Polym. 2014;102:691-698.
27. Vivek Dave, Renu Bala Y, Shipra G, Swapnil S. Guggulosomes: A herbal approach for enhanced topical delivery of phenylbutazone. Fut J Pharm Sci. 2017; 3:23-32.
28. Hirpara MR, Manikkath J, Sivakumar K, et al. Long circulating PEGylated-chitosan nanoparticles of rosuvastatin calcium: Development and *in vitro* and *in vivo* evaluations. Int J Biol Macromol. 2018;107: 2190-2200.
29. Sternby B, Hartmann D, Borgstrom B, Nilsson A. Degree of *in vivo* inhibition of human gastric and pancreatic lipases by Orlistat (Tetrahydrolipstatin, THL) in the stomach and small intestine. Clin Nutr. 2002;21(5):395-402.
30. Castillo F, Gonzalez DR, Moore-Carrasco R. Effects of *Phaseolus vulgaris* extract on lipolytic activity and differentiation of 3T3-L1 preadipocytes into mature adipocytes: A strategy to prevent obesity. J Nutr Metab; 2019.
DOI: 10.1155/2019/5093654
31. Dolenc A, Govedarica B, Dreu R, Kocbek P. Nanosized particles of orlistat with enhanced *in vitro* dissolution rate and lipase inhibition. Int J Pharm. 2010;396(1-2):149-155.

Peer-review history:
The peer review history for this paper can be accessed here:
http://www.sdiarticle4.com/review-history/66721